

Flux-to-voltage characteristic simulation of superconducting nanowire interference device*

Xing-Yu Zhang(张兴雨)^{1,2}, Yong-Liang Wang(王永良)^{1,3,†}, Chao-Lin Lv(吕超林)^{1,3}, Li-Xing You(尤立星)^{1,2,3,‡}, Hao Li(李浩)^{1,3}, Zhen Wang(王镇)^{1,3}, and Xiao-Ming Xie(谢晓明)^{1,3}

¹State Key Laboratory of Functional Material for Informatics, Shanghai Institute of Microsystem and Information Technology, Chinese Academy of Sciences (CAS), Shanghai 200050, China

²Center of Materials Science and Optoelectronics Engineering, University of Chinese Academy of Sciences, Beijing 100049, China

³CAS Center for Excellence in Superconducting Electronics, Shanghai 200050, China

(Received 9 March 2020; revised manuscript received 8 April 2020; accepted manuscript online 7 May 2020)

Inspired by recent discoveries of the quasi-Josephson effect in shunted nanowire devices, we propose a superconducting nanowire interference device in this study, which is a combination of parallel ultrathin superconducting nanowires and a shunt resistor. A simple model based on the switching effect of nanowires and fluxoid quantization effect is developed to describe the behavior of the device. The current–voltage characteristic and flux-to-voltage conversion curves are simulated and discussed to verify the feasibility. Appropriate parameters of the shunt resistor and inductor are deduced for fabricating the devices.

Keywords: superconducting nanowire, switching effect, flux-to-voltage conversion, interference device

PACS: 85.25.Am

DOI: 10.1088/1674-1056/ab90f4

1. Introduction

The conventional superconducting quantum interference device (SQUID) usually comprises a macroscopic superconducting loop with Josephson junctions (JJs), through which the supercurrent passes by quantum-mechanical tunneling.^[1] Owing to the fluxoid quantization in the superconducting loop and Josephson tunneling in JJs, the SQUID voltage is sensitive to tiny changes in applied magnetic field. Therefore, it becomes one of the most sensitive magnetic detectors, which has been widely used in magnetometers, magnetoencephalography, and scanning SQUID microscope. In the past decades, many researchers managed to develop interference devices beyond the traditional superconductor–insulator–superconductor (SIS) junctions, such as nanoSQUIDs using Dayem nanobridges,^[2,3] the one-dimensional superconducting ring that utilizes phase slips in mesoscopic superconducting rings,^[4] for catering to the applications such as high-precision magnetic spin detection and quantum imaging.

In 1982, Fink *et al.* proposed a new type of SQUID based on a homogeneous mesoscopic superconducting loop, whose width and thickness were much smaller than Ginzburg–Landau coherence length.^[5,6] In 1993, the critical current oscillation was demonstrated in a mesoscopic superconducting aluminum loop without artificial weak links.^[7] Similar behavior was also demonstrated in various forms of superconducting loops and nanowire networks, verifying the fluxoid quantization in a su-

perconducting loop and feasibility of SQUIDs without JJs. These studies focused on manipulating the superconducting phase, which aimed at realizing an actual planar SQUID. In recent years, a step structure in current–voltage (I – V) characteristics was demonstrated in nanowire devices with an external shunt resistor while driving with an rf source, which is similar to Shapiro steps, but actually results from the phase-locking between the external rf drive source and local thermal relaxation oscillations.^[8,9] In comparison with the mesoscopic devices, these devices are based on the fast thermal relaxation rather than a Josephson effect,^[10,11] which is promising to implement the novel devices based on nanowires. In the recent work by Toomey *et al.*, the influence of resistive shunting on nanowires was discussed in detail.^[12] Some superconducting devices using this quasi-Josephson effect, like the memory element, were fabricated for non-destructive readout,^[13–15] providing the possibility of bridging the gap between nanowires and Josephson junctions.

In this study, we propose a superconducting nanowire interference device with nanowires instead of Josephson junctions, based on the fluxoid quantization effect and switching effect of nanowires. This device comprises two parallel ultrathin superconducting nanowires and an external shunt resistor. Comparing with the previous studies, we introduce the fluxoid quantization effect in simulation, discuss the feasibility of direct readout via nanowire loop, and simulate the interference

*Project supported by the National Key Research and Development Program of China (Grant No. 2017YFA0304000), the National Natural Science Foundation of China (Grant Nos. 61671438 and 61827823), the Science and Technology Commission of Shanghai Municipality, China (Grant No. 18511110200), and the Program of Shanghai Academic/Technology Research Leader, China (Grant No. 18XD1404600).

†Corresponding author. E-mail: wangyl@mail.sim.ac.cn

‡Corresponding author. E-mail: lxyou@mail.sim.ac.cn

phenomenon based on the switching effect of nanowires. An equivalent circuit model is presented to analyze its working principles. The I - V and flux-to-voltage transfer characteristics are studied via numerical simulations. Simulation results show that the periodical flux-to-voltage characteristics are similar to those of the conventional SQUIDs, proving the feasibility of a novel nanowire interference device.

2. Model and simulation

In comparison with the conventional dc-SQUIDs, the novel nanowire interference device replaces JJs with nanowires and utilizes the switching effect of nanowires. For verifying its feasibility, it is vital to understand the operating mechanism. In this section, we build a model of nanowires based on the switching effect mechanism at first. Then, the superconducting loop of nanowires is analyzed by taking the fluxoid quantization effect into consideration. Finally, a feasible nanowire interference device shunted with a resistor is presented, and its I - V and flux-to-voltage characteristics are simulated.

2.1. Model of nanowire loop

2.1.1. Model of single nanowire

The dynamics of current-biased nanowires can be qualitatively understood as the interaction between electrical and thermal systems as discussed in a previous study.^[16] In this paper, we use the lumped-element model, which consists of an inductor L_k arising from the kinetic motion of the superconducting Cooper pairs and a switch in parallel with the resistance R_{hs} ,^[17,18] to describe the electrothermal interaction process of nanowires, *i.e.*, superconducting state, hotspot state, and normal state, as shown in Fig. 1(a).

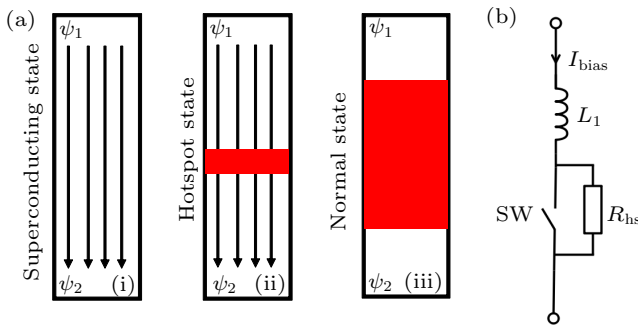


Fig. 1. (a) Three states of nanowire: (i) superconducting state, (ii) hotspot state, (iii) normal state (“latched” state). $\psi_{1,2}$ denotes the wave function at both ends of the nanowire. (b) Schematic diagram of simplified nanowire model. L_1 denotes the inductance of nanowire. R_{hs} represents the resistance of hotspot region in hotspot state. SW refers to the switching effect of nanowires. SW is open for hotspot state, while closed for superconducting state.

The superconducting state occurs when the entire wire remains in the superconducting phase, whereas the nanowire behaves like an inductor, which is mostly due to the kinetic energy of a Cooper pair rather than geometric inductance.^[19]

When the current through the nanowire exceeds its switching current I_{sw} , a hotspot appears and quickly forms a resistive region across the nanowire, which is known as the hotspot state. In the hotspot state, the formation of the hotspot is simply modeled as the opening of the switch. The hotspot grows due to the Joule heating and thermal diffusion, and eventually stagnates for the combined effects of heating, diffusion, and thermal relaxation to the substrate.^[17,20] When the bias current becomes significantly large, the thermal energy exceeds the thermal relaxation capability between the nanowire and the substrate, then the nanowire latches and switches into the normal state. Although there are many outstanding researches of the detailed physics of the formation and growth of the hotspot region,^[21,22] it is reasonable to disregard microscopic physics when the emphasis is placed on the macroscopic behavior of nanowires. In this study, we do not discuss the short and complicated evolution process of the hotspot, and we use the lumped-element model as shown in Fig. 1(b). When the current through the nanowire exceeds its switching current I_{sw} , the switch is open, *i.e.*, the resistance of the hotspot region is equal to constant R_{hs} . The switch is closed and the resistance is equal to zero when the current is below the retrapping current I_{re} , denoting the superconducting state. The switching effect can be described as follows:

$$SW = \begin{cases} \text{open,} & i > I_{sw}, \text{ hotspot state,} \\ \text{closed,} & i < I_{re}, \text{ superconducting state.} \end{cases} \quad (1)$$

2.1.2. Model of loop

In the conventional dc-SQUIDs, two JJs are connected in parallel to form a superconducting loop as first demonstrated in 1964 by Jaklevic *et al.*^[23] In the present study, JJs are replaced with two nanowires as shown in Fig. 2(a), which is similar to the geometry of the standard nanobridge SQUID.^[24] An equivalent circuit based on the switching model of nanowires is shown in Fig. 2(b), where $SW_{1,2}$ denotes the state of nanowires as shown in Eq. (1), $i_{1,2} = I_{bias}/2 \pm i_{flux}$ denotes the current through two parallel nanowires respectively, I_{bias} is the current through parallel nanowires and i_{flux} is the circular current resulting from the external magnetic flux Φ_e applied to the device. When both $SW_{1,2}$ are closed, *i.e.*, both nanowires are superconducting, the sum of the fluxoid should be quantized in units of Φ_0 , according to the fluxoid quantization formula,^[25] *i.e.*, $\Phi_{loop} = \Phi_e + \Phi_{NW} = n\Phi_0$, where Φ_0 is the flux quanta and equals the Planck constant h divided by the electron charge e , *i.e.*, $\Phi_0 = h/(2e) \approx 2.07 \times 10^{-15}$ Wb. Parameter n is the quantum number and must be an integer, Φ_e is the external magnetic flux, and Φ_{NW} is the self-generated flux, which equals $(L_1 \cdot i_1 - L_2 \cdot i_2)$ according to the explanation of Fulton.^[26] The current through two parallel nanowires $i_{1,2}$ equals $I_{bias}/2 \pm i_{flux}$. Thus, when $L_1 = L_2$, we have

$$n\Phi_0 - (L_1 + L_2) \cdot i_{flux} = \Phi_e, \quad (2)$$

where $L_{1,2}$ denotes the inductance of the nanowires forming the superconducting loop. Then, the circular current in the superconducting loop i_{flux} and the switching current of the nanowire loop $I_{\text{sw,loop}}$ can be written as $i_{\text{flux}} = (n\Phi_0 - \Phi_e)/(L_1+L_2)$, and $I_{\text{sw,loop}} = 2 \cdot (I_{\text{sw}} - |i_{\text{flux}}|)$ respectively. It

should be noted that the circular current i_{flux} should be less than the switching current of a single nanowire I_{sw} to keep the superconducting state, *i.e.*, $|n\Phi_0 - \Phi_e|/(L_1+L_2) \leq I_{\text{sw}}$, which limits the choice of n . In our simulation, the allowed value of n is 0, according to the parameters listed in Table 1.

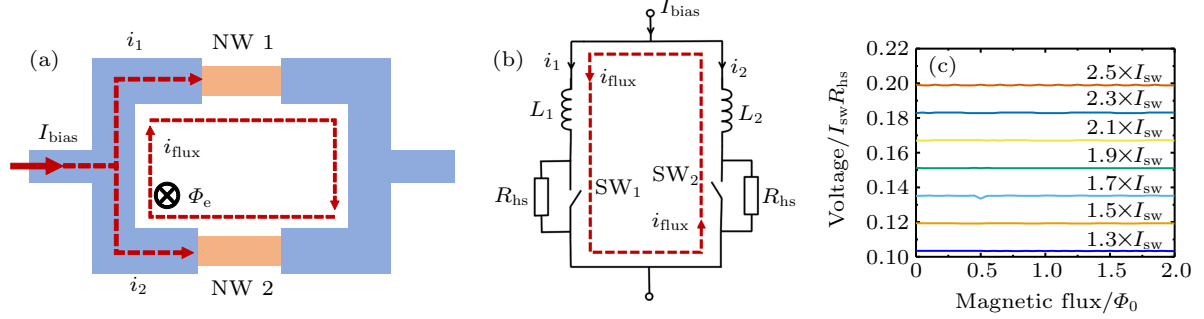


Fig. 2. (a) Schematic diagram of two parallel ultrathin superconducting nanowires. I_{bias} is the current through parallel nanowires, $i_{1,2}$ denote the currents in nanowires, and i_{flux} represents the circulating current due to external magnetic flux Φ_e . The direction of circulation depends on fluxoid number n . (b) Equivalent circuit of parallel nanowires based on switch model. $L_{1,2}$ denotes nanowire's inductance. $\text{SW}_{1,2}$ represents the switching effect of the nanowire. $\text{SW}_{1,2}$ is open for hotspot state with hotspot resistance R_{hs} , while closed for superconducting state. (c) Simulation results of flux-to-voltage conversion curves for different curves increase from $1.3 \cdot I_{\text{sw}}$ to $2.5 \cdot I_{\text{sw}}$ in steps of $0.2 \cdot I_{\text{sw}}$ from bottom to top. Modulation disappears due to the latching effect.

Numerical methods are used to solve the above equations and obtain output voltage curves across the device as shown in Fig. 2(c). The used parameters are listed in Table 1. The inductance of nanowires is 160 pH and the switching current is 10 μA . These data are estimated from a ~ 7 -nm-thick, 80-nm-wide, and 160-nm-long niobium nitride (NbN) film deposited on SiO_2 .^[27] The hotspot resistance R_{hs} of nanowires is normalized in the simulation, which is usually a few hundred ohms.^[16,28] Simulation results show that the flux-to-voltage conversion does not occur in parallel nanowires, and the voltage across the parallel nanowires is linear with respect to the bias current. This is due to the fact that the nanowires are difficult to recover the superconducting state, which is called the latching effect. When I_{bias} slightly exceeds the switching current of one nanowire, the hotspot forms due to the current redistribution caused by the magnetic flux applied to the superconducting loop. However, the inductive time constant, which governs the resetting of the current after hotspot formation, is quite shorter than the time for the hotspot to cool, which makes the nanowire stay in the normal state.^[29] This “latched” state remains until the current through the nanowire is lower than its retrapping current I_{re} . Thus, in a parallel nanowire loop, the external flux Φ_e cannot continuously modulate the output voltage to implement the interference behavior, *i.e.*, to achieve a stable flux-to-voltage conversion characteristic.

Table 1. Simulation parameters for device.

Variable	Parameter	Simulation value
$L_{1,2}$	inductance of nanowires	160 pH
I_{sw}	switching current of nanowires	10 μA
R_{hs}	resistance of nanowires	/
R_{shunt}	shunt resistance	$0.03 \cdot R_{\text{hs}}$
L_{shunt}	shunt inductance	~ 10 pH

2.2. Model of nanowire interference device

To avoid the latching phenomenon, a small-value resistor is connected in parallel with nanowires, as reported previously,^[12,30] to enhance the thermal relaxation of nanowires and make the switching effect of superconducting nanowires stable. When the nanowire switches out of the superconducting state, the shunt resistor can provide another path to divert the bias current, which is sufficient to restrict the growth of the hotspot and allow nanowires to recover the superconducting state more rapidly. As emphasized in previous studies,^[12,31] the parasitic inductance also has a significant effect on the nonlinear response of the shunted system, which is necessary to take it into consideration in our simulation. The device is schematically shown in Fig. 3(a), where it can be seen that the external resistor R_{shunt} and inductor L_{shunt} are used in parallel nanowires.

The schematic diagram of the simplified device model is shown in Fig. 3(b), where parallel nanowires form a superconducting loop with the shunt inductor and resistor connected in parallel. Based on the switching model discussed above, the device can be described as follows:

$$\begin{cases}
 I_{\text{bias}} = i_1 + i_2 + i_3, & L = L_1 = L_2, \\
 L \frac{di_1}{dt} + \gamma_1 R_{\text{hs}} i_1 = L \frac{di_2}{dt} + \gamma_2 R_{\text{hs}} i_2, \\
 L \frac{di_1}{dt} + \gamma_1 R_{\text{hs}} i_1 = L_{\text{shunt}} \frac{di_3}{dt} + R_{\text{shunt}} i_3,
 \end{cases} \quad (3)$$

where the superconducting nanowire is modeled as a switch resistance in series with the kinetic inductance, $\gamma_{1,2}$ is equal to 1 for the hotspot state, while it is 0 for the superconducting state, $i_{1,2,3}$ denote the current through the two branches of nanowire loop, and the shunt resistor respectively, $L_{1,2}$ denotes the inductance of nanowires, while L_{shunt} is the external

inductance. R_{hs} and R_{shunt} denote the resistance of the hotspot state and shunt resistor respectively. In the nanowire loop, the nanowire is switched into the hotspot state when the current $i_{1,2} = I_{\text{bias}}/2 \pm i_{\text{flux}}$ exceeds the switching current I_{sw} , and remains in the resistive state until $i_{1,2}$ drops below the retrapping current I_{re} .

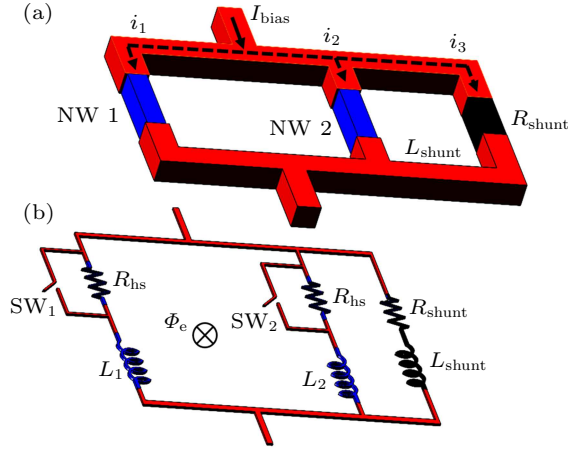


Fig. 3. (a) Schematic diagram of the nanowire interference device with a shunt resistor. It comprises two parallel ultrathin superconducting nanowires shunted with resistor R_{shunt} . External inductance L_{shunt} is taken into consideration to estimate the effect of parasitic parameters. Φ_e is the external magnetic flux applied to the device. $i_{1,2,3}$ denote the currents through the parallel nanowires and the shunt resistor respectively. (b) Equivalent circuit of the device with a shunt resistor. Φ_e is the external magnetic flux applied to the device. $L_{1,2}$ denote the inductances of nanowires. $\text{SW}_{1,2}$ denote the switching effect of nanowires. $\text{SW}_{1,2}$ is open for hotspot state with hotspot resistance of R_{hs} , while it is closed for the superconducting state.

Via solving Eqs. (2) and (3) with the parameters listed in Table 1, the I - V characteristics at $\Phi_e = 0$ and $0.5\Phi_0$ are obtained and demonstrated in Fig. 4(a). The shunt resistance in simulation is set to be $0.03 \cdot R_{\text{hs}}$, while the shunt inductance is assumed to be approximately 10 pH. By changing the value of the magnetic flux applied to the superconducting loop for $I_{\text{re}} = 0.3 \cdot I_{\text{sw}}$, the flux-to-voltage conversion curves are simulated for a device with different bias currents, and the results are shown in Fig. 4(b). The bias currents of the flux modulation curves increase from $1.1 \cdot I_{\text{sw}}$ to $2.5 \cdot I_{\text{sw}}$ in steps of $0.2 \cdot I_{\text{sw}}$ from bottom to top. It is noticeable that the shunt resistor can efficiently suppress the latching effect, and for a given bias current, the periodic and symmetric flux modulation curve is similar to that in the conventional SQUID. Since the fluxoid in the superconducting loop is quantized in units of the flux quanta Φ_0 , the applied magnetic flux can be treated as a kind of perturbation, which can redistribute the current through two nanowires, denoted as $i_{1,2} = I_{\text{bias}}/2 \pm i_{\text{flux}}$. When the bias current is low, it is difficult for the magnetic flux applied to the superconducting loop to disturb the superconducting nanowire and push it into the hotspot state. As the bias current exceeds the switching current I_{sw} of the single nanowire, this perturbation becomes obvious. The use of the shunt resistor helps nanowires dissipate the heat and recover the superconducting state in a short time, which avoids the latching effect at the

higher bias current, and makes the interference stable. However, when the bias current is significantly large, exceeding the suppression of the shunt resistor, both nanowires will latch, and the interference effect will be broken by the thermal effect. These simulation results indicate that the flux-to-voltage conversion, *i.e.*, periodical interference effect, can be obtained in a planar nanowire loop via using suitable shunting. The interference phenomenon in nanowire interference device is governed by nonlinearly switching from the superconducting state to a hotspot state due to thermal heating and the fluxoid quantization effect in the superconducting loop, which is different from the tunneling of Cooper pairs in Josephson junction-based device.

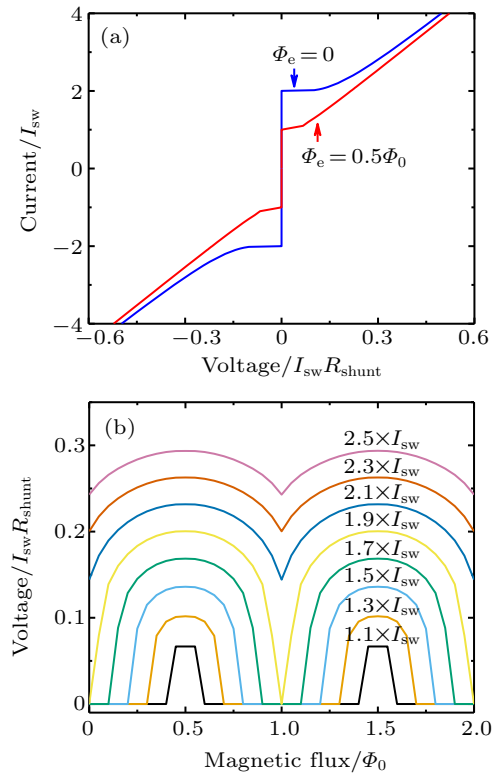


Fig. 4. (a) Simulation results of current-voltage characteristic with a shunt resistor. Bias current is normalized by switching current of single nanowire I_{sw} , and output voltage is normalized by the multiplication of switching current and shunt resistance. (b) Simulation results of flux-to-voltage conversion curves. Bias currents of flux modulation curves increase from $1.1 \cdot I_{\text{sw}}$ to $2.5 \cdot I_{\text{sw}}$ in steps of $0.2 \cdot I_{\text{sw}}$ from bottom to top. Each curve has periodicity and symmetry.

3. Discussion

To implement a practical device and pave the way for fabrication, some parameters need further discussing. The shunt resistor is used to limit the growth of the hotspot, and ensure the recovery of the superconducting state and stable interference effect. We change the values of the shunt resistor into $0.01 \cdot R_{\text{hs}}$, $0.05 \cdot R_{\text{hs}}$, $0.1 \cdot R_{\text{hs}}$, $0.15 \cdot R_{\text{hs}}$, and $0.25 \cdot R_{\text{hs}}$ respectively, whereas other parameters listed in Table 1 are fixed for $I_{\text{bias}} = 2 \cdot I_{\text{sw}}$. It is discovered that the flux-voltage conversion curve becomes steeper and the modulation depth is enhanced when the shunt resistance increases as shown

in Fig. 5(a). However, when the resistance is changed to a larger value ($0.25 \cdot R_{hs}$), the flux-to-voltage effect disappears due to the latching effect. This shows that a small shunt resistor is indispensable for the switch dynamics of the nanowire and interference effect. On the other hand, the inductance of nanowires is also important. It is set to be 16.5, 66, 100, 165, 230 pH separately, while the other parameters are also fixed for $I_{bias} = 2 \cdot I_{sw}$. The obtained modulation curves are shown in Fig. 5(b). Simulation results show that a smaller inductance of the nanowire leads to a steeper and more drastic modulation because the modulation strength of the applied magnetic flux depends on nanowire inductance, *i.e.*, $\Delta I = \Phi_0 / (L_1 + L_2)$. Thus, the modulation becomes larger for smaller inductance.

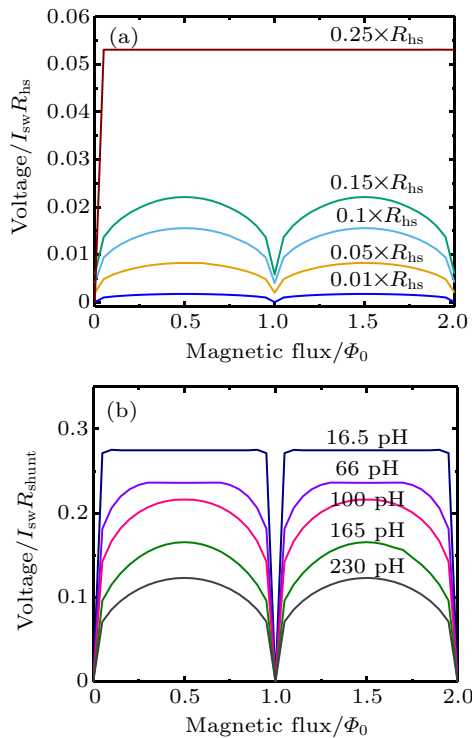


Fig. 5. Flux-to-voltage conversion curves for devices with different values of shunt resistance and nanowire inductance. (a) Curves for different values of shunt resistance. Shunt resistances are selected to be $0.01 \cdot R_{hs}$, $0.05 \cdot R_{hs}$, $0.1 \cdot R_{hs}$, $0.15 \cdot R_{hs}$, and $0.25 \cdot R_{hs}$ respectively from bottom to top for $I_{bias} = 2 \cdot I_{sw}$. Output voltage is normalized by the multiplication of switching current and hotspot resistance. For a smaller resistor, device can support higher bias current, but output voltage is lower. When resistance becomes larger, device is easier to latch. (b) Flux-to-voltage conversion curves for different values of nanowire inductance of 16.5, 66, 100, 165, 230 pH, respectively, for $I_{bias} = 2 \cdot I_{sw}$. Output voltage is normalized by the multiplication of switching current and shunt resistance. As the inductance of nanowire decreases, modulation curve becomes steeper, while output voltage slightly increases.

The parameters of shunt resistance and nanowire inductance have been discussed above, which can be easily realized in fabrication. The shunt resistor can be fabricated via using molybdenum (Mo) film with a sheet resistance of approximately 1Ω at cryogenic temperature (4.2 K).^[32] The inductance can be realized by a 7-nm-thick NbN film deposited on SiO_2 , whose sheet inductance is about $100 \text{ pH}/\square$.^[28] For smaller inductance, recent work by McCaughan *et al.* reported

that the kinetic inductance per square of about 10-nm-thick niobium deposited on sapphire is $3.7 \text{ pH}/\square$ with a switching current of $175 \mu\text{A}$.^[33] A 5-nm-thick magnesium diboride (MgB_2) film grown on 6H-SiC also shows the kinetic inductance of $1.6 \text{ pH}/\square$ at cryogenic temperature (5 K), which is several tens times lower than that of the NbN film.^[34] These researches promise to more flexible and easy fabrication of the low-inductance nanowires.

Comparing with the conventional SQUIDs, the planar fabrication process and compatibility with existing nanowire electronics make it easier to implement the nano-sized superconducting loops and the large-scale integration. The switching effect of nanowires will contribute to the high-output voltage, which helps to increase the signal-to-noise ratio. In contrast with the existing nanowire-based devices, we introduce the fluxoid quantization effect and discuss the feasibility of direct readout and interference effect via simulation. However, the speed of the device is limited by the thermal time constant of the material due to the dependence on nanowires' switching effect. The shunt resistance should be tuned to balance the speed voltage and the output voltage. In addition, the routing of the signals should be taken into consideration in the case of the large-scale implementation. The device proposed in this work has the potential to realize the interference effect and large-scale integration. It may be helpful to the readout of detectors, like superconducting nanowire single-photon detectors and transition-edge sensors.^[35,36]

4. Conclusions

In this work, we propose a superconducting nanowire interference device based on the switching effect of nanowires and the fluxoid quantization effect in a superconducting nanowire loop. The proposed device replaces the Josephson junctions in a SQUID with resistively shunted nanowires. A simplified lumped-element model of nanowires, combining with fluxoid quantization in the superconducting loop, is developed to simulate the real-time behavior of current and voltage across the device. The flux-to-voltage characteristics are also obtained through numerical simulation, proving the feasibility of the planar interference nanowire devices. The parameters of the nanowire inductance and shunt resistor are discussed and proved to be feasible for devices' fabrication.

Acknowledgment

The authors would like to thank Zhang W, Wang H, Hu P, and Huang J for fruitful discussion.

References

- [1] Clarke J and Braginski A I 2004 *SQUID Handbook, Vol. 1, Fundamentals and technology of SQUIDs and SQUID systems* (Wiley-VCH)

- [2] Granata C and Vettoliere A 2016 *Phys. Rep.* **614** 1
- [3] Liu X, Liu X, Wang H, Chen L and Wang Z 2015 *Physica C* **515** 36
- [4] Petkovic I, Lollo A, Glazman L I and Harris J G 2016 *Nat. Commun.* **7** 13551
- [5] Fink H, López A and Maynard R 1982 *Phys. Rev. B* **26** 5237
- [6] Fink H, Grünfeld V and López A 1987 *Phys. Rev. B* **35** 35
- [7] Moshchalkov V, Gielen L, Dhallé M, Van Haesendonck C and Bruynseraede Y 1993 *Nature* **361** 617
- [8] Hadfield R H, Miller A J, Nam S W, Kautz R L and Schwall R E 2005 *Appl. Phys. Lett.* **87** 203505
- [9] You L X, Liu D K and Yang X Y (Chinese Patent) 102694117A [2015-08-19]
- [10] Brenner M W, Roy D, Shah N and Bezryadin A 2012 *Phys. Rev. B* **85** 224507
- [11] Liu D K, You L X, Chen S J, Yang X Y, Wang Z, Wang Y L, Xie X M and Jiang M H 2013 *IEEE Trans. Appl. Supercond.* **23** 2200804
- [12] Toomey E, Zhao Q Y, McCaughan A N and Berggren K K 2018 *Phys. Rev. Appl.* **9** 064021
- [13] Toomey E, Onen M, Colangelo M, Butters B A, McCaughan A N and Berggren K K 2019 *Phys. Rev. Appl.* **11** 034006
- [14] McCaughan A N, Toomey E, Schneider M, Berggren K K and Nam S W 2019 *Supercond. Sci. Technol.* **32** 015005
- [15] Onen M, Turchetti M, Butters B A, Bionta M R, Keathley P D and Berggren K K 2020 *Nano Lett.* **20** 664
- [16] Yang J K W, Kerman A J, Dauler E A, Anant V, Rosfjord K M and Berggren K K 2007 *IEEE Trans. Appl. Supercond.* **17** 581
- [17] Nicolich K L, Cahall C, Islam N T, Lafyatis G P, Kim J, Miller A J and Gauthier D J 2019 *Phys. Rev. Appl.* **12** 034020
- [18] Berggren K K, Zhao Q Y, Abebe N S, Chen M, Ravindran P, McCaughan A N and Bardin J 2018 *Supercond. Sci. Technol.* **31** 055010
- [19] Kerman A J, Dauler E A, Keicher W E, Yang J K W, Berggren K K, Gol'tsman G and Voronov B 2006 *Appl. Phys. Lett.* **88** 111116
- [20] Kerman A J, Yang J K W, Molnar R J, Dauler E A and Berggren K K 2009 *Phys. Rev. B* **79** 100509
- [21] Engel A, Renema J J, Il'in K and Semenov A 2015 *Supercond. Sci. Technol.* **28** 114003
- [22] Sidorova M, Semenov A, Hubers H W, Charaev I, Kuzmin A, Doerner S and Siegel M 2017 *Phys. Rev. B* **96** 184504
- [23] Jaklevic R, Lambe J, Silver A and Mercereau J 1964 *Phys. Rev. Lett.* **12** 159
- [24] Hazra D 2019 *Phys. Rev. B* **99** 144505
- [25] Deaver B S and Fairbank W M 1961 *Phys. Rev. Lett.* **7** 43
- [26] Fulton T A 1970 *Solid State Commun.* **8** 1353
- [27] Zhu D, Colangelo M, Korzh B A, Zhao Q Y, Frasca S, Dane A E, Velasco A E, Beyer A D, Allmaras J P and Ramirez E 2019 *Appl. Phys. Lett.* **114** 042601
- [28] Yang X, You L, Zhang L, Lv C, Li H, Liu X, Zhou H and Wang Z 2018 *IEEE Trans. Appl. Supercond.* **28** 1
- [29] Annunziata A J, Quaranta O, Santavicca D F, Casaburi A, Frunzio L, Ejrnaes M, Rooks M J, Cristiano R, Pagano S, Frydman A and Prober D E 2010 *J. Appl. Phys.* **108** 084507
- [30] Liu D K, Chen S J, You L X, Wang Y L, Miki S, Wang Z, Xie X M and Jiang M H 2012 *Appl. Phys. Express* **5** 125202
- [31] Biswas S, Winkelmann C B, Courtois H, Dauxois T, Biswas H and Gupta A K 2018 arXiv: 1807.07720v3 [cond-mat.supr-con]
- [32] Makise K, Terai H and Zhen W 2012 *Phys. Proc.* **36** 116
- [33] McCaughan A N, Zhao Q and Berggren K K 2016 *Sci. Rep.* **6** 28095
- [34] Cherednichenko S, Acharya N, Novoselov E and Drakinskiy V 2019 arXiv: 1911.01480 [cond-mat.supr-con]
- [35] Shen X F, Yang X Y, You L X 2010 *Chin. Phys. Lett.* **27** 087404
- [36] Liu J, Xiao L, Liu Y, Cao L and Shen Z 2019 *Chin. Phys. B* **28** 028504